AGU PUBLICATIONS

Geophysical Research Letters

RESEARCH LETTER
10.1002/2013GL058886

Key Points:
- Simulated spontaneous outer rise and wedge events agree geometrically with nature
- Stress transfer and dynamic Coulomb wedge theory explain their occurrence
- They increase megathrust event recurrence and complexity, and tsunami hazard

Supporting Information:
- Readme
- Figure S1 and Table S1

Correspondence to:
Y. van Dinther,
ylona.vandinther@erdw.ethz.ch

Citation:
van Dinther, Y., P. M. Mai, L. A. Dalguer, and T. V. Gerya (2014), Modeling the seismic cycle in subduction zones: The role and spatiotemporal occurrence of off-megathrust earthquakes, *Geophys. Res. Lett.*, *41*, 1194–1201, doi:10.1002/2013GL058886.

Received 2 DEC 2013
Accepted 30 JAN 2014
Accepted article online 4 FEB 2014
Published online 27 FEB 2014

Modeling the seismic cycle in subduction zones: The role and spatiotemporal occurrence of off-megathrust earthquakes

Y. van Dinther[1,2], P. M. Mai[3], L. A. Dalguer[1], and T. V. Gerya[2]

[1]Swiss Seismological Service, ETH Zürich, Zürich, Switzerland, [2]Institute of Geophysics, ETH Zürich, Zürich, Switzerland, [3]Division of Physical Sciences and Engineering, KAUST, Thuwal, Saudi Arabia

Abstract Shallow off-megathrust subduction events are important in terms of hazard assessment and coseismic energy budget. Their role and spatiotemporal occurrence, however, remain poorly understood. We simulate their spontaneous activation and propagation using a newly developed 2-D, physically consistent, continuum, viscoelastoplastic seismo-thermo-mechanical modeling approach. The characteristics of simulated normal events within the outer rise and splay and normal antithetic events within the wedge resemble seismic and seismological observations in terms of location, geometry, and timing. Their occurrence agrees reasonably well with both long-term analytical predictions based on dynamic Coulomb wedge theory and short-term quasi-static stress changes resulting from the typically triggering megathrust event. The impact of off-megathrust faulting on the megathrust cycle is distinct, as more both shallower and slower megathrust events arise due to occasional off-megathrust triggering and increased updip locking. This also enhances tsunami hazards, which are amplified due to the steeply dipping fault planes of especially outer rise events.

1. Introduction

Between 1976 and 2007 approximately 45% of the seismic moment release in subduction zones occurred at the megathrust interface [*Presti et al.*, 2012]. Seismic moment released by off-megathrust earthquakes attains approximately 41% within the oceanic slab (of which 64% in the shallowest 70 km) and 14% within the overriding plate. Besides introducing unconventional seismic hazard, off-megathrust events are important for tsunami hazard assessment [e.g., *Satake and Tanioka*, 1999], assessing seismic cycle maturity [e.g., *Lay et al.*, 1989], and understanding faulting mechanics [*McGuire and Beroza*, 2012]. Their spatiotemporal occurrence, however, remains insufficiently understood. The objective of this study is to demonstrate that self-consistent seismo-thermo-mechanical numerical modeling of these events contributes to understanding their spatiotemporal occurrence and their impact on the megathrust seismic cycle.

Thus far, spontaneous seismic cycle models in subduction zones do not yet include off-fault events or plasticity, although the importance off-fault plasticity is confirmed by field observations [*Baker et al.*, 2013]. Several seismic cycle models include (a) a predefined branching fault [e.g., *Duan and Oglesby*, 2007], (b) off-fault plasticity, but with kinematically prescribed seismic cycles on normal faults [*Dempsey et al.*, 2012], or (c) a continuum damage rheology to represent off-fault seismicity in strike-slip settings [e.g., *Lyakhovsky and Ben-Zion*, 2008]. However, the applied a priori definition of an (off-megathrust) fault plane geometry and ad hoc stresses might affect rupture propagation. This makes the spontaneous numerical development of (new) shear localizations and a mesoscopic fault structure crucial [e.g., *Ando and Yamashita*, 2007].

This study explores a new, virtually quasi-static seismic cycle model that includes Drucker-Prager plasticity and spontaneous off-megathrust events governed by strongly rate-dependent friction. We use the viscoelastoplastic continuum seismo-thermo-mechanical model (STM) validated for seismic cycle applications against a laboratory model [*van Dinther et al.*, 2013a] and natural observations [*van Dinther et al.*, 2013b]. This seismo-thermo-mechanical approach includes the physically consistent evolution of stress, strength, temperature, and geometry of specific rupture paths and the lithosphere. Results presented in this study agree with spatial seismic and seismological observations and analytical predictions from dynamic Coulomb

©2014. American Geophysical Union. All Rights Reserved.

wedge theory [*Wang and Hu*, 2006]. They also reveal that off-megathrust events have a distinct impact on the megathrust seismic cycle.

2. Seismo-Thermo-Mechanical Modeling

We employ the 2-D, continuum, viscoelastoplastic code I2ELVIS [*Gerya and Yuen*, 2007]. Extensions for seismo-thermo-mechanical modeling are validated and explained in *van Dinther et al.* [2013a, 2013b]. This single-framework model uses a finite difference scheme on a fully staggered Eulerian grid in combination with a Lagrangian marker-in-cell technique. We then implicitly solve the conservation of mass, momentum, and energy for an incompressible medium with a viscoelastoplastic rheology. The momentum equations include the inertial term to stabilize high-coseismic slip rates at low time steps. A time step of 5 years, however, reduces our formulation to a virtually quasi-static one. Ruptures during the resulting events hence represent the occurrence of rapid threshold-exceeding slip during which permanent displacement and stress drop occur along a localized interface [*van Dinther et al.*, 2013b].

The brittle/plastic faulting process is simulated by a Drucker-Prager plastic yielding model in which the second invariant of the deviatoric stress tensor is limited at each Lagrangian rock marker by a pressure-dependent yield stress σ_{yield}

$$\sigma_{yield} = C + \mu \cdot (1 - \lambda) \cdot P, \tag{1}$$

where C is cohesion, μ is the effective rate-dependent friction coefficient, λ is a fixed pore fluid pressure factor (P_{fluid}/P), and P is pressure. Yielding and local stress-strain rate equilibrium are achieved by reducing the effective viscosity, thereby weakening the material and localizing deformation. Brittle instabilities and subsequent healing are introduced, both on- and off-megathrust, by a strongly rate-weakening friction coefficient [e.g., *Burridge and Knopoff*, 1967; *Cochard and Madariaga*, 1994]

$$\mu = \mu_s(1 - \gamma) + \mu_s \frac{\gamma}{1 + \frac{V}{V_c}}. \tag{2}$$

Here γ denotes the amount of rate-induced weakening equivalent to $1 - \mu_d/\mu_s$, and $-(\alpha - \beta)/\mu_s$. μ_s and μ_d are the static and minimum dynamic friction coefficient and α and β quantify a direct and evolution effect, respectively [*Ampuero and Ben Zion*, 2008]. The viscoplastic slip rate V, which is normalized by the characteristic slip rate V_c, is calculated as the velocity difference between two interfaces spaced one grid step apart, i.e., the viscoplastic strain rate σ_{yield}/η times the grid size dx. This local, invariant formulation allows for spontaneous localization at any orientation. The spontaneous rupture paths are governed by local stress and strength states instead of being a priori defined.

The model is setup as a 1500×200 km^2 trench-normal section of the Southern Chilean active continental margin (Figure 1a). During 5.1 million years, an oceanic slab of age 40 Ma is driven at 7.5 cm/yr below a sedimentary wedge and continental overriding plate into the upper mantle (Figure S1a in the supporting information).

The viscoelastoplastic thermomechanical parameters of these lithologies are based on a range of laboratory experiments (Table S1 in the supporting information). The weakest, top 2 km of oceanic crust forms the megathrust interface. Its velocity weakening frictional formulation is parameterized using $\gamma = 0.7$, $V_c = 4.4$ cm/yr, $C = 6$ MPa, and $\lambda = 0.95$, as justified in *van Dinther et al.* [2013b]. A transition to velocity strengthening friction with $\gamma = -1.5$ and $V_c = 6.3$ cm/yr occurs from 150°C to 100°C. The frictional parameters for other lithologies are simplified to the same velocity weakening parameters, while only tailoring static (and hence dynamic) friction coefficients to each lithology (Table S1 in the supporting information).

3. Spatial Characteristics of Off-Megathrust Seismicity

Besides interplate slip transients akin to earthquake ruptures on the megathrust interface [*van Dinther et al.*, 2013b], we observe three types of off-megathrust faulting. Below we describe the normal faulting events in the outer rise and the forethrust splay and normal antithetic faults in the fore arc separately.

3.1. Outer Rise Normal Faults

The variability of outer rise normal faults is evident from the viscoplastic strain rates active over a 1000 year period (Figure 1b). Outer rise localizations related to slab bending extend from ~70 km seaward to ~50 km landward of the trench. They occur with a quasi-regular spacing of on average 3–4 km. When occurring beneath the trench, they dip landward at 60°–68° (or its conjugate angle) toward the neutral stress horizon

©2014. American Geophysical Union. All Rights Reserved.

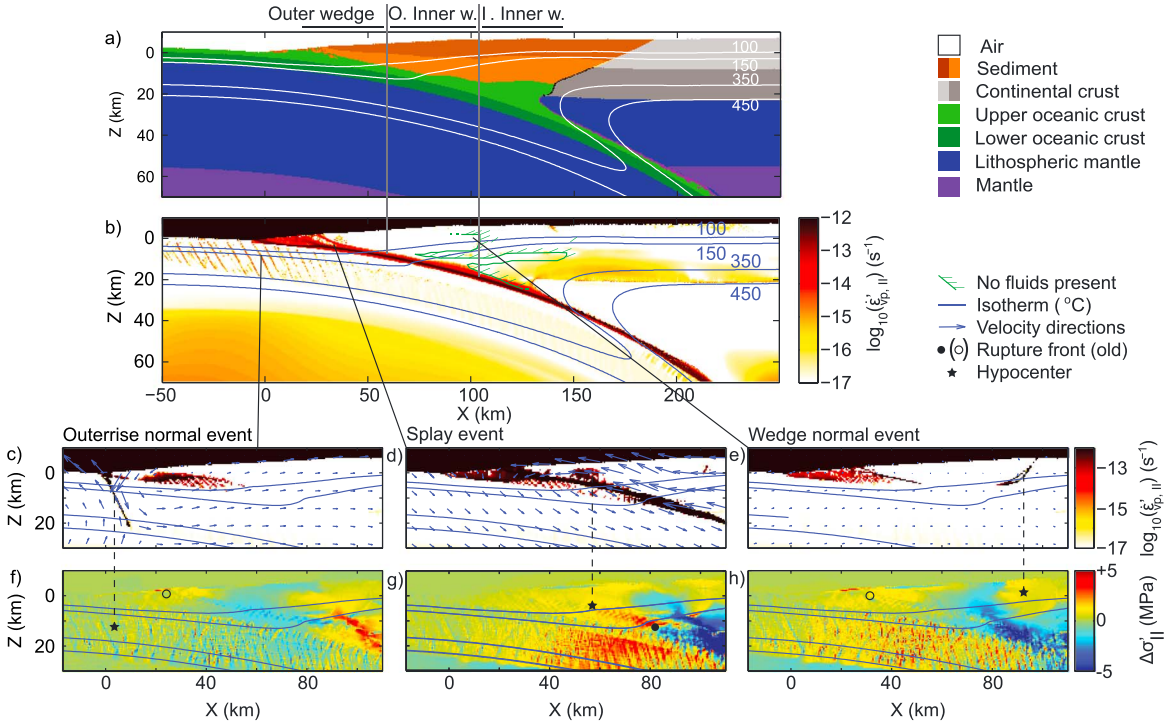

Figure 1. (a) Zoom of the initial model setup in terms of lithology and temperature (see Figure S1 in the supporting information for complete setup). (b) Long-term off-megathrust activity for 1000 year time steps (when slip rate-dependent friction is not effective) in terms of second invariant of the deviatoric viscoplastic strain rate. (c–e) Spatiotemporal zooms of the current model for similar strain rates overlain by velocities (arrows) at the peak of reference off-megathrust events. (f–h) Second invariant deviatoric stress change of a moment just prior to off-megathrust initiation with respect to the start of the triggering thrust event. X is distance landward from the trench; Z is depth below the trench.

at 25 km below the trench. In the reference model with small time steps, the largest outer rise normal faulting event shows particularly large vertical seafloor surface velocities (arrows in Figure 1c). This leads to larger than expected vertical seafloor displacements of 13 m upward and 25 m downward. Regular megathrust events, on the contrary, have near-field differential uplifts of on average 10 m. The larger than ever observed seafloor displacements are facilitated by self-consistent slab pull through gravity and the steeply dipping fault planes, which enhance tsunami hazards [e.g., *Satake and Tanioka*, 1999; *Wendt et al.*, 2009].

Besides these large surface displacements, all spatial characteristics of outer rise normal faulting induced by slab bending, arising spontaneously in our physics-based simulations, agree with seismic and seismological observations [e.g., *Forsyth*, 1982; *Masson*, 1991; *Ranero et al.*, 2003]. The dip of the conjugate faults (60°–68°) approximately corresponds to the internal friction angle ϕ with respect to a vertical maximum compressive stress, as expected for extensional outer rises [*Warren et al.*, 2007]. Observed dips, however, vary around 45° [*Ranero et al.*, 2003], although a dip of 59°, close to our simulation results, is suggested for the 2007 *M*8.1 Kuril normal faulting event [*Ammon et al.*, 2008]. These features are in general agreement with observations from long-term, static simulations [e.g., *Naliboff et al.*, 2013].

3.2. Splay Faults in the Sedimentary Wedge

Splay faults or forethrusts come up from the megathrust interface within the outer wedge with velocity strengthening friction applied at the basal interface (Figure 1b). Internal strength decreases within this tip of the fore arc, as the wedge thins and pressure decreases. Dips of different forethrust planes decrease from ~28° at the velocity strengthening transition (Figure 1d) to subhorizontal with fan-like faulting in the thin frontal prism near the trench. These spontaneous spatial characteristics agree with splay faults revealed in seismic images [e.g., *Moore et al.*, 2007; *Kimura et al.*, 2007].

3.3. Antithetic Normal Faults in the Sedimentary Wedge

Within the hydrated outer part of the inner wedge (O. Inner w. in Figures 1a and 1b), we occasionally observe a megathrust earthquake that triggers initially relatively steep (~51°), listric, antithetic normal faults near the slope break (Figure 1e). Similar type of normal faulting is observed in response to the 2010 *M*8.8 Maule earthquake at roughly 100 km from the trench as well [e.g., *Farias et al.*, 2011]. The proximity of these

©2014. American Geophysical Union. All Rights Reserved.

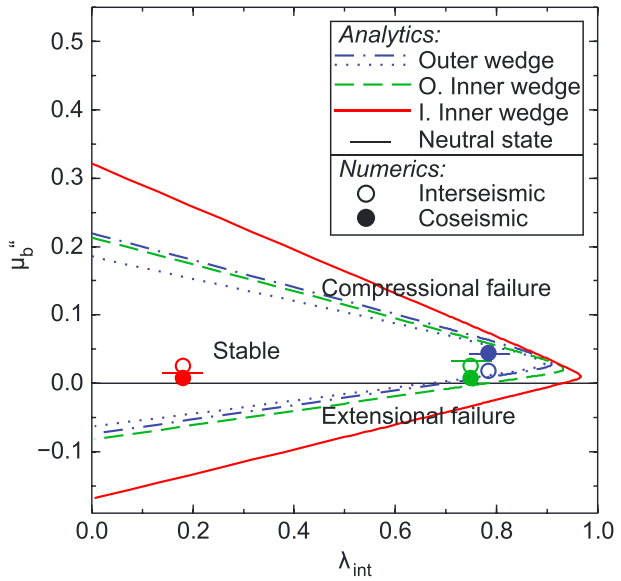

Figure 2. Comparison to dynamic Coulomb wedge theory [*Wang and Hu*, 2006] by showing the critical values of effective basal friction μ_b'' ($=\mu_b(1-\lambda_b)$) as a function of average pore fluid pressure factor (fluid pressure divided by solid pressure) in the internal wedge λ_{int} for three spatial regions (shown in Figure 1b). Critical and neutral states are calculated from the following values: Outer wedge has $\alpha = 3.0°$, $\beta = 9.2°$, $\lambda_{int} = 0.78$, and $\mu_{int} = 0.35$ for interseismic dash-dotted line and $\mu_{int} = 0.30$ for coseismic dotted line that has internal frictional weakening as well; Outer part of inner wedge has $\alpha = 2.2°$, $\beta = 10°$, $\lambda_{int} = 0.75$, and $\mu_{int} = 0.36$; and Inner part of inner wedge has $\alpha = 1.2°$, $\beta = 19°$, $\lambda_{int} = 0.18$, and $\mu_{int} = 0.38$.

events to coastal cities suggests they should be considered in seismic hazard assessment [*Farias et al.*, 2011].

4. Stress Transfer and Dynamic Coulomb Wedge Theory

An off-megathrust event typically occurs when two criteria are met: (a) the long-term (or initial) stress state (Figure S1c in the supporting information) should be close to failure and (b) a trigger provides the final increase of the stress to the strength over an area larger than the nucleation size.

The exact timing of an off-megathrust event is determined by this latter triggering component, which is typically due to the quasi-static stress transfer following a megathrust event (section 5). This mechanism is supported by the off-megathrust hypocenter being within the region of increase of the second invariant of the stress tensor (star in Figures 1f–1h). Within the outer rise a megathrust event enhances shallow slab bending and hence increases extensional slab stresses by up to 1 MPa (Figure 1f). The seaward motion of the wedge compresses the outer wedge and thereby facilitates thrusting on splay faults (Figure 1g). In the wake of the megathrust rupture the wedge is extended, thereby locally increasing extensional stresses (Figure 1h).

Whether quasi-static stress transfer is able to successfully trigger a certain type of off-megathrust event depends on the long-term stress and strength states. Classical Coulomb wedge theory analytically describes the mechanics of a plastic accretionary wedge on the verge of Coulomb failure, while sliding over a basal frictional decollement [e.g., *Davis et al.*, 1983; *Dahlen et al.*, 1984]. It predicts the basal and internal strengths required to deform the wedge, and which type of plastic failure occurs where to retain a critical taper (or cone shape). This theory is extended to a dynamic, elastic version for time scales of seismic cycles by including temporal variations of basal friction coefficients [*Wang and Hu*, 2006].

For comparison to this dynamic Coulomb wedge theory we divide the sedimentary wedge in three sections (Figures 1a and 1b): (a) the outer wedge underlain by a velocity strengthening interface, (b) the outer part of the inner wedge, where fluids distinctly weaken the wedge, and (c) the inner part of the inner wedge, where fluids are largely absent within the wedge. For each of these regions Figure 2 shows the analytical predictions for the critical values of effective basal friction μ_b'' at which compressional and extensional failure occurs (colored lines) as a function of internal pore fluid pressure factor λ_{int}. These critical states, and their corresponding neutral ones, are calculated from each regions average surface slope α, basal dip β, and internal strength (λ_{int} and μ_{int}).

The observed faulting types within these regions (Figures 1c–1e), and the absence of faulting, correspond approximately to these analytical predictions from dynamic Coulomb wedge theory. The outer wedge (blue) progresses from being near extensional failure within the interseismic period (open dot) to reaching a state of being at the verge of compressional Coulomb failure, as rapid slip induces a strengthened basal interface (filled dot). The outer part of the inner wedge (green) is interseismically stable. However, as the rupture reduces the interface's frictional strength, such wedge surface topography can no longer be sustained. Consequently, extensional failure could occur. The long-term background extensional regime results from a weak interface and a weak wedge due to high pore fluid pressures ($\lambda = 0.95$) [*Seno*, 2009; *van Dinther et al.*,

©2014. American Geophysical Union. All Rights Reserved.

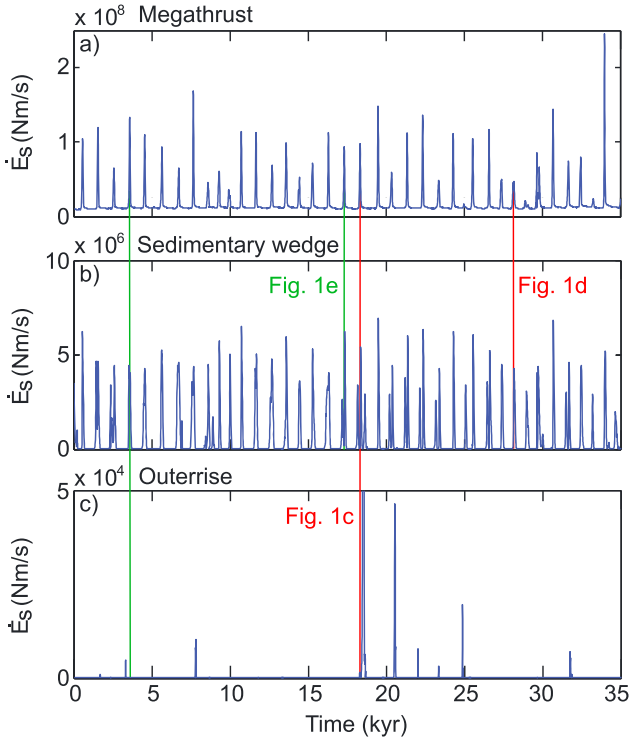

Figure 3. Temporal relation between (a) megathrust, (b) wedge, and (c) outer rise seismicity evident from the dissipated strain energy rate $\dot{E}_s$ per area through time (note that vertical scales in Figures 3a–3c are different, and the maximum reached in Figure 3c is 8.8×10^5 Nm/s). Areas are automatically determined at each time step based on lithology (upper oceanic crust, sediment, and lithospheric mantle, respectively) and location. Lines delineate example temporal relations. Red indicates triggering by the main thrust, while green indicates triggering of the thrust by off-megathrust events.

2013b]. Furthermore, it might depict transient deformation from a higher cohesion configuration used in *van Dinther et al.* [2013b]. The stronger inner part of the inner wedge (red) is predicted to remain stable throughout all phases of the seismic cycle. Indeed, no plastic failure is observed in this part. Corresponding to predictions of the neutral state for this setup, the stress state typically changed from compressionally stable to extensionally stable.

The approximate agreement confirms both the applicability of dynamic Coulomb wedge theory [*Wang and Hu*, 2006] and our implementation of plasticity, faulting, and topography evolution. By also including a variation of internal friction parameters, i.e., decreasing friction in the outer wedge during coseismic failure as shown with the blue dotted line in Figure 2, the agreement would be improved further. Even higher consistency between these models is inhibited by averaging of variable strength properties and invalid analytical assumptions on a small-angle approximation in a wedge without cohesion.

5. Temporal Characteristics of Off-Megathrust Seismicity

An overview of temporal relations between the megathrust, sedimentary wedge, and outer rise is provided by the evolution of each regions dissipated strain energy rate (Figure 3). This is calculated as the viscoplastic strain rate multiplied by the nondeviatoric stress components and integrated over a volume selected based on lithology.

In this specific strongly coupled setup about 92% of the coseismically dissipated strain energy is released on the megathrust interface (Figure 3a). Megathrust activity dictates energy dissipation within the sedimentary wedge (Figure 3b) and oceanic slab (Figure 3c). A plastic response in the sedimentary wedge, responsible for ~7.5% of coseismic dissipation, typically follows thrust dissipation by approximately four time steps. However, about 30% of the megathrust events are actually preceded by brittle/plastic localizations within the wedge as well. Approximately 10% of wedge events occur independently. An important role for splay fault propagation and wedge failure is also anticipated in nature. Several recent megathrust earthquakes are suggested to have propagated on splay faults to some extent [e.g., *DeDontney et al.*, 2011; *Tsuji et al.*, 2011].

The triggering of deeper outer rise events, which dissipate about 0.05% of the total coseismic energy, is less common as they follow only ~14% of the megathrust events (Figure 3b). They are also delayed more and cross correlations show that they, on average, occur 39 time steps after the megathrust event. We also observe three outer rise events that tentatively hasten the occurrence of a premature megathrust event.

The observed temporal relations between outer rise and main thrust activity agree with various examples of recent earthquakes. The quasi-static release of stress and the accelerated motion of the slab has been

©2014. American Geophysical Union. All Rights Reserved.

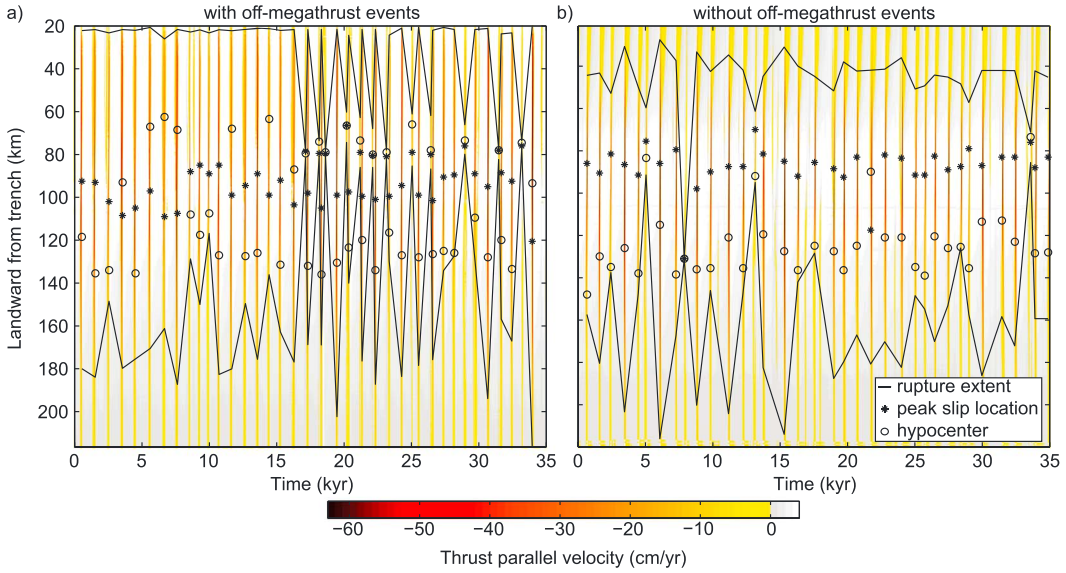

Figure 4. Impact of off-megathrust events on megathrust cyclicity. Spatiotemporal evolution of thrust-parallel velocity at 6.4 km above the highest strain rate thrust interface for (a) the reference model with off-megathrust events (C_{off} = 6 MPa) and (b) the reference model without off-megathrust events (C_{off} = 200 MPa) [from Figure 4a in *van Dinther et al.*, 2013b]. Black shapes in the legend result from a velocity threshold of −15.6 cm/yr.

observed to trigger a megathrust event (e.g., the 2009 Samoa-Tonga earthquakes) [*Lay et al.*, 2010]. On the other hand, in 2006–2007 unlocking of the megathrust transferred extension due to slab pull updip and triggered an extensional event within the outer rise (central Kuril doublet) [*Ammon et al.*, 2008]. The dominant occurrence of outer rise normal events at the beginning of the seismic cycle confirms the hypothesis that outer rise events could give an indication of the temporal maturity of the seismic cycle [e.g., *Lay et al.*, 1989]. The observed quasi-static stress transfer into the outer rise, as plate bending is enhanced, also agrees with kinematic calculations of extensional stress changes [e.g., *Dmowska et al.*, 1988]. These findings support the concept of increased seismic and tsunami hazard, once a thrust or outer rise earthquake occurred.

6. Impact on Megathrust Cycling

The impact of these off-megathrust events and off-megathrust plastic energy dissipation on megathrust seismicity is analyzed by comparing the spatiotemporal evolution of thrust-parallel velocity for a model with (Figure 4a; C_{off} = 6 MPa) and without off-megathrust events (Figure 4b; C_{off} = 200 MPa, taken from *van Dinther et al.* [2013b]). Thrust-parallel velocities are shown at 6.4 km above the highest strain rate interface. A velocity threshold at 3.8 times the reversed interseismic velocity (−15.6 cm/yr) is used to determine source parameters [*Corbi et al.*, 2013; *van Dinther et al.*, 2013a, 2013b]. In these figures white regions indicating strong interseismic locking, gray regions indicating more aseismic creep, and vertical red to black lines show rapid slip transients akin to earthquakes.

The largest impact of off-megathrust yielding is observed in the low-temperature updip part, where updip locking is extended from landward of ~70 km to from ~40 km onward. A lowered coseismic displacement velocity (as also seen in, e.g., *Andrews* [2005]) reduces the efficiency of updip velocity strengthening in inhibiting the rupture. This reduces the updip coseismic yield strength and prolongs the rupture to almost up to the trench. Subsequently, aseismic creep is reduced, leading to more updip locking and a wider observed seismogenic zone. This results from stresses that are lowered even below their already reduced strength, since yielding of the shallow wedge contributes to the coseismic release of updip interface stresses. The effect of a lowered coseismic slip rate is reversed in the velocity weakening region in which higher coseismic strengths reduce stresses less. This leads to a smaller strength excess in the shallow part of the seismogenic zone, which leads to more frequent nucleation near the updip limit. Shallower nucleation is moreover increased by occasional premature triggering of megathrust events by sedimentary wedge events. Both these phenomena reduce the recurrence interval of megathrust events.

©2014. American Geophysical Union. All Rights Reserved.

Off-megathrust plastic yielding leads to a minor reduction in seismic energy dissipated at the megathrust over time (~3%). This percentage is lower than expected from single-dynamic rupture studies [e.g., *Ma*, 2012], since megathrust events occurred more frequently. Dissipated megathrust energies are also increased by more shallow coseismic slip due to updip off-megathrust yielding and updip extension of interseismic locking due limited slip speeds.

Off-megathrust events also increase the complexity of the long-term megathrust seismicity pattern measured using the coefficient of variation *Cv*, i.e., the standard deviation over the average of a distribution [e.g., *Kuehn et al.*, 2008]. We find that *Cv* increases from ~0.3 without off-megathrust events to 0.44 and 0.55 with them, for recurrence interval and overriding displacement, respectively. This increase of complexity mainly results from more frequent updip nucleation.

7. Conclusions

The seismo-thermo-mechanical geodynamic modeling approach was extended with off-megathrust plasticity and corresponding events to analyze their poorly understood role and spatiotemporal occurrence. Off-megathrust events are shown to distinctly affect the megathrust cycle by increasing the amount of recurring events and updip hypocenters through their occasional premature triggering of megathrust ruptures. Locking updip of the seismogenic zone is also extended. This leads to shallower ruptures that could enhance tsunami hazard. Seafloor displacements are also increased by the steeply dipping off-megathrust fault planes, especially those from outer rise events.

Spatial and temporal characteristics of spontaneously rupturing outer rise normal, splay, and antithetic normal faults resemble natural observations and examples of recently observed earthquake interactions. The occurrence of off-megathrust wedge events can be explained by quasi-static stress changes on top of a long-term stress state compatible with failure once basal friction variations are included according to dynamic Coulomb wedge theory. This theory correctly predicts where and which type of wedge-internal faulting events can and cannot occur.

Acknowledgments

We thank an anonymous reviewer for his supportive review. We also thank Sean Willett, Francesca Funiciello, and Alice Gabriel for stimulating discussions. Kelin Wang and Yan Hu are thanked for providing input and feedback on dynamic Coulomb wedge theory. This research was supported by SNSF grant 200021-125274.

The Editor thanks one anonymous reviewer for his/her assistance in evaluating this paper.

References

Ammon, C., H. Kanamori, and T. Lay (2008), A great earthquake doublet and seismic stress transfer cycle in the central Kuril islands, *Nature*, *451*, 561–565.

Ampuero, J.-P., and Y. Ben Zion (2008), Cracks, pulses and macroscopic asymmetry of dynamic rupture on a bimaterial interface with velocity weakening friction, *Geophys. J. Int.*, *173*, 674–692.

Ando, R., and T. Yamashita (2007), Effects of mesoscopic-scale fault structure on dynamic earthquake ruptures: Dynamic formation of geometrical complexity of earthquake faults, *J. Geophys. Res.*, *112*, B09303, doi:10.1029/2006JB004612.

Andrews, D. J. (2005), Rupture dynamics with energy loss outside the slip zone, *J. Geophys. Res.*, *110*, B01307, doi:10.1029/2004JB00319.

Baker, A., R. W. Allmendinger, L. A. Owen, and J. A. Rech (2013), Permanent deformation caused by subduction earthquakes in northern Chile, *Nat. Geosci.*, *6*(6), 492–496.

Burridge, R., and L. Knopoff (1967), Model and theoretical seismicity, *Bull. Seismol. Soc. Am.*, *57*(3), 341–371.

Cochard, A., and R. Madariaga (1994), Dynamic faulting under rate-dependent friction, *Pure Appl. Geophys.*, *142*(3/4), 419–445.

Corbi, F., F. Funiciello, M. Moroni, Y. van Dinther, P. M. Mai, L. A. Dalguer, and C. Faccenna (2013), The seismic cycle at subduction thrusts: 1. Insights from laboratory models, *J. Geophys. Res. Solid Earth*, *118*, 1483–1501, doi:10.1029/2012JB009481.

Dahlen, F., J. Suppe, and D. Davis (1984), Mechanics of fold-and-thrust belts and accretionary wedges: Cohesive Coulomb theory, *J. Geophys. Res.*, *89*, 10,087–10,101.

Davis, D., J. Suppe, and F. Dahlen (1983), Mechanisms of fold-and-thrust belts and accretionary wedges, *J. Geophys. Res.*, *88*(21-22), 1153–1172.

DeDontney, N., J. R. Rice, and R. Dmowska (2011), Influence of material contrast on fault branching behavior, *Geophys. Res. Lett.*, *38*, L14305, doi:10.1029/2011GL047849.

Dempsey, D. E., S. M. Ellis, J. V. Rowland, and R. A. Archer (2012), The role of frictional plasticity in the evolution of normal fault systems, *J. Struct. Geol.*, *39*, 122–137.

Dmowska, R., J. Rice, L. Lovison, and D. Josell (1988), Stress transfer and seismic phenomena in coupled subduction zones during the earthquake cycle, *J. Geophys. Res.*, *93*, 7869–7884.

Duan, B., and D. D. Oglesby (2007), Nonuniform prestress from prior earthquakes and the effect on dynamics of branched fault systems, *J. Geophys. Res.*, *112*, B05308, doi:10.1029/2006JB004443.

Farias, M., D. Comte, S. Roecker, D. Carrizo, and M. Pardo (2011), Crustal extensional faulting triggered by the 2010 Chilean earthquake: The Pichilemu Seismic Sequence, *Tectonics*, *30*(6), TC6010, doi:10.1029/2011TC002888.

Forsyth, D. (1982), Determinations of focal depths of earthquakes associated with the bending of oceanic plates at trenches, *Phys. Earth Planet. Inter.*, *28*, 141–160.

Gerya, T., and D. Yuen (2007), Robust characteristics method for modelling multiphase visco-elasto-plastic thermo-mechanical problems, *Phys. Earth Planet. Inter.*, *163*(1-4), 83–105.

Kimura, G., Y. Kitamura, Y. Hashimoto, A. Yamaguchi, T. Shibata, K. Ujiie, and S. Okamoto (2007), Transition of accretionary wedge structures around the up-dip limit of the seismogenic subduction zone, *Earth Planet. Sci. Lett.*, *255*(3), 471–484.

Kuehn, N. M., S. Hainzl, and F. Scherbaum (2008), Non-Poissonian earthquake occurrence in coupled stress release models and its effect on seismic hazard, *Geophys. J. Int.*, *174*(2), 649–658.

©2014. American Geophysical Union. All Rights Reserved.

Lay, T., L. Astiz, H. Kanamori, and D. Christensen (1989), Temporal variation of large intraplate earthquakes in coupled subduction zones, *Phys. Earth Planet. Inter.*, *54*(3-4), 258–312.

Lay, T., C. J. Ammon, H. Kanamori, L. Rivera, K. D. Koper, and A. R. Hutko (2010), The 2009 Samoa-Tonga great earthquake triggered doublet, *Nature*, *466*, 964–970.

Lyakhovsky, V., and Y. Ben-Zion (2008), Scaling relations of earthquakes and aseismic deformation in a damage rheology model, *Geophys. J. Int.*, *172*(2), 651–662.

Ma, S. (2012), A self-consistent mechanism for slow dynamic deformation and large tsunami generation for earthquakes in the shallow subduction zone, *Geophys. Res. Lett.*, *39*, L11310, doi:10.1029/2012GL051854.

Masson, D. G. (1991), Fault patterns at outer trench walls, *Mar. Geophys. Res.*, *13*, 209–225.

McGuire, J. J., and G. C. Beroza (2012), A rogue earthquake off Sumatra, *Science*, *336*(6085), 1118–1119.

Moore, G., N. Bangs, A. Taira, S. Kuramoto, E. Pangborn, and H. Tobin (2007), Three-dimensional splay fault geometry and implications for tsunami generation, *Science*, *318*, 1128–1131.

Naliboff, J. B., M. I. Billen, T. Gerya, and J. Saunders (2013), Dynamics of outer rise faulting in oceanic-continental subduction systems, *Geochem. Geophys. Geosyst.*, *14*(7), 2310–2327, doi:10.1002/ggge.20155.

Presti, D., A. Heuret, F. Funiciello, and C. Piromallo (2012), A new database on subduction seismicity at the global scale, Abstract EGU2012-2277 presented at 2012 EGU General Assembly, Vienna, Austria, 22-27 April.

Ranero, C. R., J. Phipps Morgan, K. McIntosh, and C. Reichert (2003), Bending-related faulting and mantle serpentinization at the Middle America trench, *Nature*, *425*(6956), 367–373.

Satake, K., and Y. Tanioka (1999), Sources of tsunami and tsunamigenic earthquakes in subduction zones, *Pure Appl. Geophys.*, *154*, 467–483.

Seno, T. (2009), Determination of the pore fluid pressure ratio at seismogenic megathrusts in subduction zones: Implications for strength of asperities and Andean-type mountain building, *J. Geophys. Res.*, *114*, B05405, doi:10.1029/2008JB005889.

Tsuji, T., Y. Ito, M. Kido, Y. Osada, H. Fujimoto, J. Ashi, M. Kinoshita, and T. Matsuoka (2011), Potential tsunamigenic faults of the 2011 off the Pacific coast of Tohoku earthquake, *Earth Planets Space*, *63*(7), 831–834.

van Dinther, Y., T. V. Gerya, L. A. Dalguer, F. Corbi, F. Funiciello, and P. M. Mai (2013a), The seismic cycle at subduction thrusts: 2. Dynamic implications of geodynamic simulations validated with laboratory models, *J. Geophys. Res. Solid Earth*, *118*, 1502–1525, doi:10.1029/2012JB009479.

van Dinther, Y., T. Gerya, L. Dalguer, P. Mai, G. Morra, and D. Giardini (2013b), The seismic cycle at subduction thrusts: Insights from seismo-thermo-mechanical models, *J. Geophys. Res. Solid Earth*, *118*, 6183–6202, doi:10.1002/2013JB010380.

Wang, K., and Y. Hu (2006), Accretionary prisms in subduction earthquake cycles: The theory of dynamic Coulomb wedge, *J. Geophys. Res.*, *111*, B06410, doi:10.1029/2005JB004094.

Warren, L., A. Hughes, and P. Silver (2007), Earthquake mechanics and deformation in the Tonga-Kermadec subduction zone from fault plane orientations of intermediate-and deep-focus earthquakes, *J. Geophys. Res.*, *112*(B5), B05314, doi:10.1029/2006JB004677.

Wendt, J., D. D. Oglesby, and E. L. Geist (2009), Tsunamis and splay fault dynamics, *Geophys. Res. Lett.*, *36*(15), L15303, doi:10.1029/2009GL038295.

©2014. American Geophysical Union. All Rights Reserved.